First Insights into the SWIRE Galaxy Populations

Carol Lonsdale

Infrared Processing & Analyis Center, California Institute of Technology, 100-22, Pasadena, CA 91125, USA

Maria del Carmen Polletta

Center for Astrophysics & Space Sciences, University of California, San Diego, La Jolla, CA 92093–0424, USA

Jason Surace, Dave Shupe, Fan Fang & C. Kevin Xu

Infrared Processing & Analyis Center, California Institute of Technology, 100-22, Pasadena, CA 91125, USA

Harding E. Smith & Brian Siana

Center for Astrophysics & Space Sciences, University of California, San Diego, La Jolla, CA 92093–0424, USA

Michael Rowan-Robinson & Tom Babbedge

Astrophysics Group, Blackett Laboratory, Imperial College, Prince Consort Road, London, SW7 2BW, UK

Seb Oliver, Francesca Pozzi & Payam Davoodi

Astronomy Centre, CPES, University of Sussex, Falmer, Brighton BN1 9QJ, UK

Frazer Owen

National Radio Astronomy Observatory, P.O. Box O, Socorro, NM 87801, USA

Deborah Padgett, Dave Frayer, Tom Jarrett, Frank Masci, JoAnne O'Linger & Tim Conrow

Infrared Processing & Analyis Center, California Institute of Technology, 100-22, Pasadena, CA 91125, USA

Duncan Farrah, Glenn Morrison & Nick Gautier

Jet Propulsion Laboratory, 264-767, 4800 Oak Grove Drive, Pasadena, CA 91109, USA

Alberto Franceschini & Stefano Berta

Dipartimento di Astronomia, Universita di Padova, Vicolo Osservatorio 5, I-35122 Padua, Italy

Ismael Perez-Fournon

Instituto de Astrofisica de Canarias, 38200 La Laguna, Tenerife, Spain

Herve Dole

Institut d'Astrophysique Spatiale, Universite Paris Sud bat 121, F-91405 Orsay, France

Gordon Stacey

Department of Astronomy, Cornell University, 220 Space Science Building, Ithaca, NY 14853, USA

Steve Serjeant

Centre for Astronomy and Planetary Science, School of Physical Sciences, University of Kent at Canterbury, Canterbury, Kent CT2 7NZ

Marguerite Pierre

CEA/DSM/DAPNIA, Service d'Astrophysique, 91191 Gif-sur-Yvette, France

Matt Griffin

Department of Physics and Astronomy, University of Wales Cardiff, 5 The Parade, Cardiff CF24 3YB, UK

Rick Puetter

Center for Astrophysics & Space Sciences, University of California, San Diego, La Jolla, CA 92093–0424, USA

ABSTRACT

We characterize the SWIRE galaxy populations in the SWIRE validation field within the Lockman Hole, based on the 3.6-24μ Spitzer data and deep U,g',r',i' optical imaging within an area $\sim$1/3 sq. deg for $\sim$16,000 Spitzer-SWIRE sources. The entire SWIRE survey will discover over 2.3 million galaxies at 3.6μm and almost 350,000 at 24μm; $\sim$ 70,000 of these will be 5-band 3.6-24μ detections. The colors cover a broad range, generally well represented by redshifted spectral

energy distributions of known galaxy populations, however significant samples of unusually blue objects in the $[3.6\text{-}4.5]\mu$m color are found, as well as many objects very red in the $3.6\text{-}24\mu$m mid-IR. Nine of these are investigated and are interpreted as star-forming systems, starbursts and AGN from z=0.37 to 2.8, with luminosities from $L_{IR}=10^{10.3}$ to $10^{13.7}$ $L_{\odot}$.

Subject headings: galaxies: evolution

1. Introduction and Observations

The Spitzer Wide-area InfraRed Extragalactic Legacy Survey, SWIRE (Lonsdale et al. 2003), will map the evolution of spheroids, disks, starbursts and AGN to z>2, within volumes large enough to sample the largest important size scales. We present initial results from deep optical (U,g',r',i') and Spitzer-SWIRE (3.6μm-24μm) imaging of 0.3 sq. deg. in the SWIRE Survey validation field (VF) in the Lockman Hole, a field selected to have extremely low cirrus emission, and a lack of bright radio sources. Deep K-band and VLA 20 cm imaging also exist, and this field will be imaged with Chandra/ACIS-I to 70ks depth in 2004 August. The full SWIRE survey will image $\sim$49 sq. deg. in all IRAC and MIPS bands in 6 fields, Area has been reduced from the strategy described by Lonsdale et al. (2003) in order to maintain two high quality coverages of each field with the MIPS 70μm array (see `http://www.ipac.caltech.edu/SWIRE` for details). The SWIRE validation field was imaged by Spitzer in December 2003 following the strategy described in Lonsdale et al. (2003), therefore it has shallower MIPS depth than the main SWIRE survey. The full SWIRE Lockman field was imaged with the new strategy in April/May 2004.

The SWIRE VF is centered at $10^h46^m, +59^d01^m$. The observations were executed on 2003 Dec 05 & Dec 09. The Spitzer PROGID for these data is 142 and the datasets are identified as IRAC: (AOR key 7770880) (AOR key 7771136) MIPS: (AOR key 7770368) (AOR key 7770624) . Data processing began with the Spizer Basic Calibrated Data products, which are individual Spitzer images corrected for bias offsets and pixel-to-pixel gain variations (flat-fielding), and flux-calibrated in surface brightness units of MJy/sr. Additional individual IRAC image processing corrected latent images and electronic offset effects. For MIPS, scan-mirror-dependent flats were derived from the data and applied to the BCD images. The individual images, which have measurable spatial distortions, were reprojected onto a single common projection system on the sky, and then coadded through averaging with outlier rejection to remove cosmic ray and other transient artifacts. A 3-color 3.6, 4.5, 24μm false color image of part of the field is shown in Plate 1.

Fluxes were extracted in 5.8″ apertures for IRAC ($\sim$2-3$\times$ the FWHM beam) and 12″ for MIPS 24μm, using SExtractor. Very few ($<$5%) of the detected objects are extended relative to the large Spitzer beams ($>$2″ at the shortest wavelength), and even fewer on scales comparable to the extraction apertures. Aperture corrections have been derived from stellar sources in the mosaicked data by the instrument teams, and these have been applied to correct to total fluxes. The IRAC flux calibration is believed to be correct within 3%, and the 24μm calibration to 10%. There is an additional scatter resulting from color dependencies in the flat field that add roughly a $<$10% random error to the fluxes for all IRAC data. The calibration was confirmed for IRAC by comparison to 2MASS, a robust extrapolation from the 2MASS K-band since the IRAC bands lie on the Rayleigh-Jeans tail of the stellar SED. For 10 stars in our field with 2MASS magnitudes, we extrapolated to a 24 micron flux density using Kurucz-Lejeune atmospheric models for MK class I, III and V implemented in the SSC's Stellar Performance Estimation Tool, assuming G5 spectral type, confirming the calibration to better than 10%. The resulting catalogs were examined by eye and remaining spurious sources (from radiation, scattered light, etc.) were removed by hand. Details of the data processing are given in Surace et al (2004) and Shupe et al. (2004).

The optical g', r' and i' data were taken in Feb, 2002 and the U data in Jan, 2004, using the MOSAIC camera on the Mayall 4m telescope at Kitt Peak National Observatory (Siana et al. 2004, in preparation). The data were processed with the Cambridge Astonomical Survey Unit's reduction pipeline following the procedures described by Babbedge et al. (2004). Fluxes were extracted within 2.06″ apertures and corrected for the aperture using profiles measured on bright stars. An analysis comparing the 2.06″ aperture-corrected magnitudes with total "Kron" magnitudes in the r' band indicated that brighter than $\sim$21.5 mag. (Vega) significant numbers of galaxies have fluxes underestimated by the aperture photometry, therefore our analysis is limited to galaxies fainter than this limit. Colors for the source samples were constructed from the aperture-corrected magnitudes.

The final depths for the Spitzer sample, at $\sim$5$\times$ the noise level, are given in Table 1. These depths are consistent with the 90% completeness limits as determined from the deviation of the observed number counts from a power law, and from simulated extractions of artificial sources injected into the data. The median achieved depths for extended objects (galaxies) in the optical bands, at the $\sim$90% completeness levels for source extraction, derived in a similar fashion to the Spitzer data, are U=24.9, g'=25.7, r'=25.0, i'=24.0.

Table 1. Spitzer Sensitivities and Detection Statistics

λ_c (μm)	3.6	4.5	5.8	8	24	3.6,4.5	All IRAC	All IRAC,24
5σ limit, validation field (μJy)	3.7	5.3	48	37.7	150	$\cdots$	$\cdots$	$\cdots$
All detections, 0.3 sq. deg., VF	16,075	12,675	1,536	1,657	1,290	11,765	950	433
Galaxies (stars removed statistically)	14,630	11,403	1,091	1,247	1,283	10,706	760	430
5σ limit, full survey (μJy)	3.7	5.3	48	37.7	106	$\cdots$	$\cdots$	$\cdots$
Predicted galaxies, 49 sq. deg. ($\times 10^6$)	2.39	1.86	0.18	0.20	0.35	1.75	0.12	0.07
Model, 49 sq. deg., Xu et al S3+E2	6.36	4.76	0.24	0.33	0.72	4.75	0.21	0.17
Projected/Model	0.38	0.39	0.75	0.61	0.49	0.37	0.57	0.41

Stars were removed statistically from the Spitzer catalog using predicted counts based on a near-infrared Galactic stellar distribution model by Jarrett et al. (1994), based on the classic optical model of Bahcall & Soneira (1980). The model was verified using optical stellarity measures for objects associated with IRAC sources, and by matching star counts within a deep 2MASS catalog which reaches ∼2 mag. fainter than the all-sky 2MASS survey (Beichman et al. 2003). Stars outnumber galaxies at F(3.6)$\gtrsim$150μJy at this latitude (Surace et al. 2004) and decrease rapidly in number relative to galaxies below that flux density.

2. Results and Discussion

The detection statistics in Table 1 indicate that over the full SWIRE survey area of ∼49 sq. deg., we will detect ∼2.4 million galaxies at 3.6μm and ∼120,000 in all 4 IRAC bands. At 24μm the detection rate for the full survey will be better than for the VF discussed here because MIPS integration time has been doubled, therefore we estimate nearly 350,000 galaxies detected in this band, and about 70,000 of these in all 4 IRAC bands as well. At optical wavelengths we detect the following numbers of sources at U$g'r'i'$ respectively: 27,911, 42,817, 39,308, 30,230, stars plus galaxies. 17,894 are detected in all 4 optical bands, and 8,626 in the combination r', 3.6, 4.5μm. 325 are detected in all 9 optical+IR bands.

We have compared the IR detection statistics to predictions from the models of Xu et al. (2003), model S3+E2, in Table 1. Model S3 includes dusty objects: spirals, starbursts and AGN; and E2 contains passively evolving stellar systems, ie. spheroids. The Xu et al. model overpredicts SWIRE IR galaxy numbers by a factor of ∼2 in the IR bands. The number counts results will be addressed by Surace et al. (2004) and Shupe et al. (2004).

Figures 1 and 2 present color-color plots which characterize the sample in g' to 24μm color-color space. Only sources detected in all four bands shown in each figure are plotted; no limits are shown for clarity. The figures show SED-redshift tracks of several galaxies with a broad range of intrinsic colors. These SEDs cover the range of colors exhibited by known objects throughout the U-24μm wavelength range and 0<z<2. We do not expect many sources in the region of the figures occupied by rare objects like Arp 220 at low redshift, because our volume coverage at low redshift space is small. A complete analysis of SWIRE galaxy colors relative to model predictions and SED-tracks is beyond the scope of this paper, requiring thorough analysis of selection effects, photometric redshifts and k-corrections. Here we note a few basic results.

There is a very broad distribution of colors in these figures. Galaxies with little on-going star formation will be relatively blue in the mid-IR due to lack of dust emission, and also

quite red in $[g' - r']$ due to domination by late-type stars, and thus found towards the lower right of Figure 1, near the elliptical SED track (red curve). Indeed, there is a concentration of systems near this region. Moreover the 3.6μm-brightest systems in the sample (blue symbols) preferentially inhabit this region, indicating that these may be relatively nearby early-type systems. The stellar tracks also cross this region of Figure 1: using the stellar model described above we predict a maximum 0.13 star fraction in the $10<$F(3.6)<150 μJy flux range, and 0.09 for $7.3<$F(3.6)<10 μJy, focused strongly within ±0.2 magnitudes of the stellar sequences. In Figure 2 the elliptical SED track lies off the figure to the bottom, due to lack of 24μm emission; objects in this lower-right area are likely to be early-type spirals or unusually dusty spheroids.

Dusty systems will be more strongly detected at the longer wavelengths, and therefore redder in the Spitzer $[3.6-4.5]$ and $[3.6-24]$ colors. There is a trend in both figures that these systems tend also to be the bluest in $[g' - r']$, inhabiting the upper left of both figures. This is expected for systems which have both young complexes of dust-enshrouded star formation dominating the mid-IR plus either (a) hot blue young stars visible in lower optical depth regions at optical wavelengths, or (b) a blue type 1 AGN visible in the optical, such as Mrk231 which tracks into this area at z>2 in Figure 2. It is notable that the most extreme systems (those toward the upper left of the figures), tend to be the fainter galaxies in the sample at 3.6μm (red symbols). This could be interpreted as due to either preferentially more distant systems or lower luminosity systems, however the complex selection and k-correction effects would need to be understood in order to investigate this further.
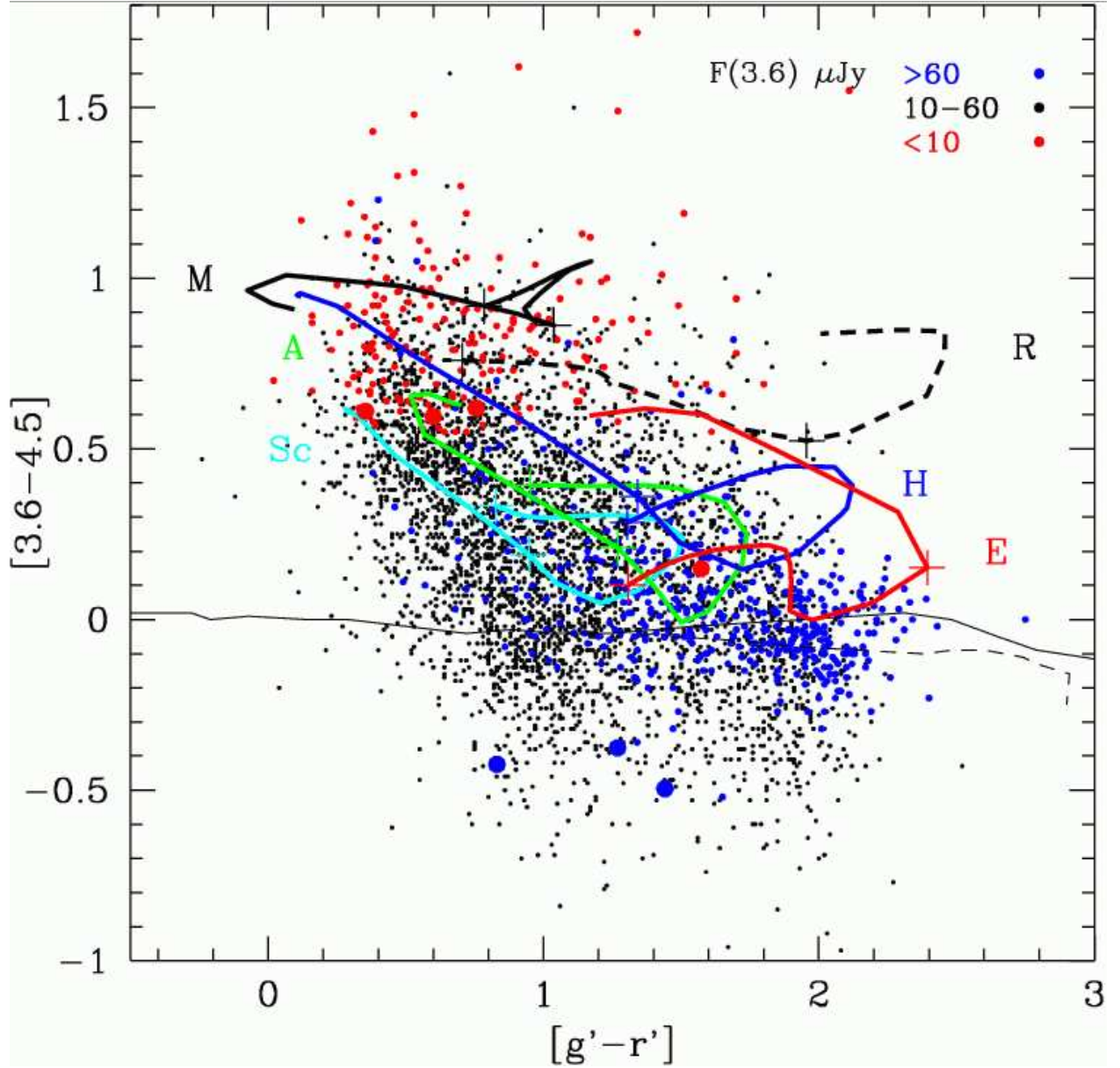
Fig. 1.— Color-color distributions for 4,395 sources detected at g', r', 3.6 and 4.5μm with S/N>10 and $r'\geq21.5$. Sources with upper limits are not shown for clarity. Stellar tracks: light black lines: main sequence solid; giants dashed; Galaxy SEDs, 0.1<z<2, with crosses at z=0.1 and z=1: elliptical (red; E); Sc spiral (cyan; Sc); Arp 220 (green; A); the well-known ULIRG & QSO Mrk 231 (black; M); an ERO, HR10 (blue; H); and a red QSO discovered in the FIRST survey (FIRST J013435.7-093102; optical/NIR spectrum from Gregg *et al.* (2002); at longer wavelengths the IR spectrum of PG1351+236, which has a very similar optical/NIR spectrum, was added by Polletta et al. 2004 (in preparation)), (dashed black: R). Units are Vega magnitudes, using zero points of 277.5, 179.5, 116.6, 63.1 & 7.3Jy at 3.6, 4.5, 5.8, 8 & 24μm respectively. Large solid dots indicate objects illustrated in Fig. 3 which are detected in each band depicted in this figure: blue symbols for objects with [3.6−4.5]< −0.3 (F(3.6)/F(4.5)>2.0) and red symbols for objects with [3.6-24]>7.5 mag (F(3.6)/F(24)<0.04).
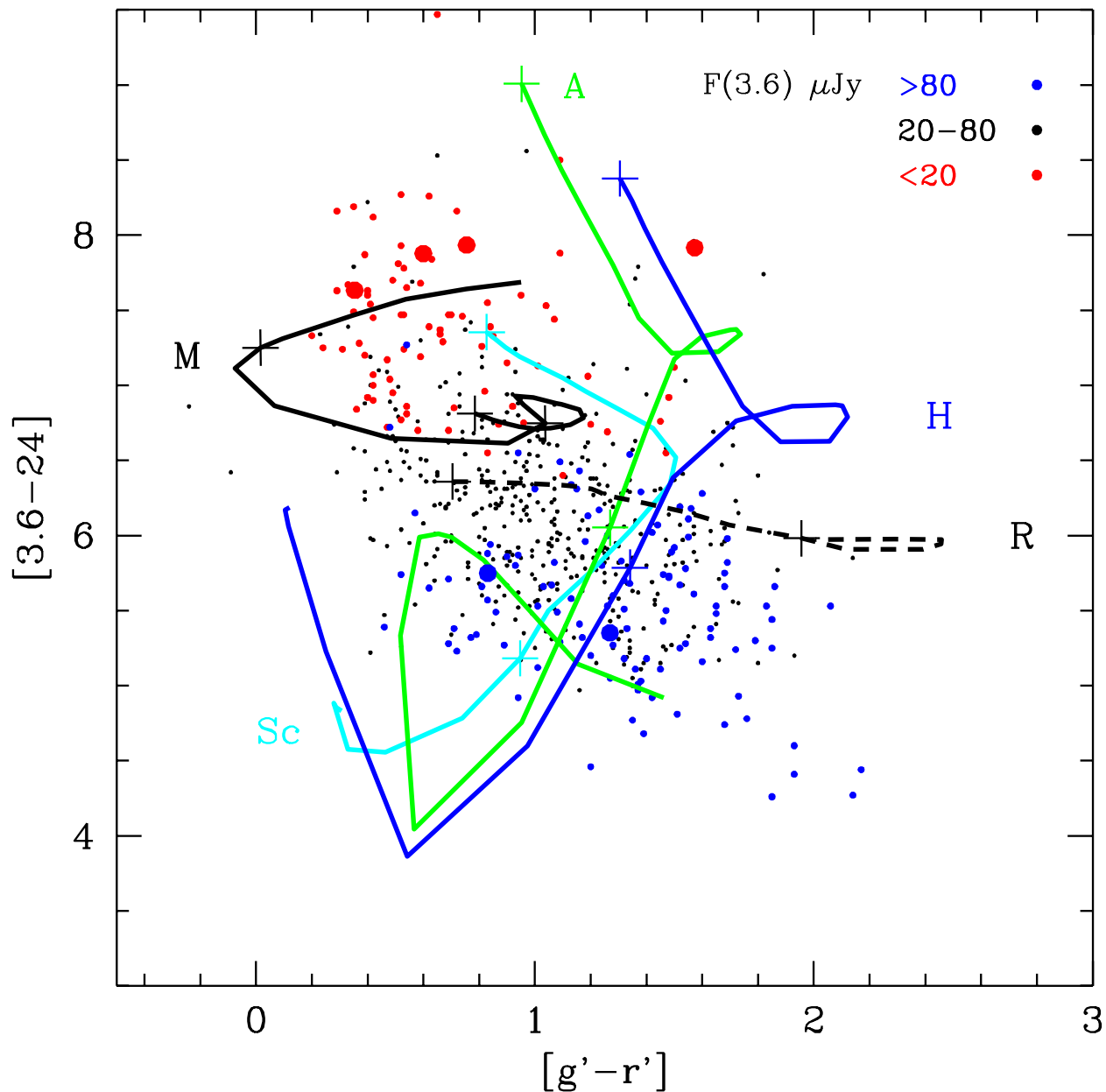
Fig. 2.— Color-color distributions for 588 sources detected at g', r', 3.6 and 24μm with S/N>5 and $r'{\geq}21.5$. Tracks and symbols are as for Figure 1, except Mrk231 has been extended to z=3 with a additional marker plotted at z=2.

Some areas of the color-color diagrams are not well covered by the SED tracks. Of particular note are some unusually blue objects in $[3.6-4.5]$, and mid-IR red sources at the upper left of Figure 2. Many additional extreme-colored objects with upper limits in one or more color are not shown in these figures. As an illustration of some of the most unusual objects populating the SWIRE sample, we have investigated a number of these sources with red $[3.6-24]$ colors and unusually blue $[3.6-4.5]$ colors, using the photometric redshift code Hyper-z (Bolzonella et al. 2000) to fit SEDs with a wide range of templates, redshifts and A_V. We used our own library (Polletta et al. 2004), the GRASIL library (Silva et al. 1998) and the Rowan-Robinson (2003) library. The Polletta et al. (2004) library contains $\sim$40 $1000\mathring{A} - 20cm$ templates for ellipticals, spirals, irregulars, starbursts, ULIRGs and AGN, derived from observed SEDs, including mid-IR ISO spectra and models following Berta et al. (2004). A more complete characterization and photometric redshift analysis of a larger SWIRE galaxy sample is in preparation (Rowan-Robinson et al. 2004).

Investigating first the blue sources, we selected 603 sources with $[3.6-4.5]< -0.3$, significantly bluer than normal galaxies and stars, with S/N$\geq$10 in both bands. Fluxes were remeasured by hand for 193 of these objects with detections in a sufficient number of bands for SED analysis. We used the IPAC-Skyview software to set background levels interactively, thus avoiding confusion with nearby sources and background contamination. 67 sources were found to have valid colors. In about 8% of the remaining cases the automated source extractor measured a different region of a close or confused pair of sources, or of an extended source, in the two bands. 32% of the sources marginally miss the color cut on careful color re-evaluation, 8% are cosmic rays or bad pixels, 36% have anomalous 3.6μm fluxes caused by local background or other effects due to bright stars, and 16% have anomalous fluxes at either 3.6 or 4.5μm with no obvious explanation. The last 3 categories represent a 76/12784=0.6% anomaly rate amongst the entire S/N>10 3.6μm catalog, and a 40% anomaly rate amongst the $[3.6-4.5]<$-0.3 sample. Since anomalies are preferentially expected amongst odd-colored sources, the high anomaly rate amongst the unusually blue sources is not unanticipated.

The 67 valid $[3.6-4.5]< -0.3$ objects exhibit a wide range of optical to mid-IR colors. 7 are relatively blue and pointlike throughout the optical and mid-IR, and are probably stars. None of the galaxy libraries contain any templates as blue as the remaining $[3.6-4.5]< -0.3$ sources at any redshift. Two objects in the literature have colors possibly as blue at 3-5μm: the peculiar QSO [HB89]0049-29 at z=0.308 (Andreani et al. 2003), and the Seyfert 2 ULIRG IRAS 00198-7826 at z=0.073 (Farrah et al. 2003). [HB89]0049-29 peaks strongly in the NIR, however it is very red from there into the optical, unlike any of our sources. IRAS 00198-7826 is not observed at these wavelengths, but is predicted to be as blue as our sources (Farrah et al. 2003), which is explained by it being a $\gtrsim$ 60Myr starburst where much of the gas and dust has been blown away by supernovae. This model for IRAS 00198-7826

can produce colors similar to those of our blue objects in the [3.6−4.5] color, but it is too blue into the optical to match any of our sources at any redshift.

Another possible explanation for the blue [3.6−4.5] colors is a strong $3.3\mu m$ PAH feature in the $3.5\mu m$ band at low redshift (<0.1), however it would have to be considerably higher equivalent width than any such feature found in any of our templates. Also possible is a strong $2.35\mu m$ CO bandhead absorption moving into the $4.5\mu m$ filter at redshift ∼0.7, requiring a young stellar population of red supergiants which is not diluted strongly by an older stellar population with a weaker absorption (Rhoads 1997). This might perhaps indicate a dominant ∼10^7 year old starburst in a fairly low mass galaxy. Alternatively such a high equivalent width may indicate low metallicity.

In Figure 3 and Table 2 we present representative best fits for 5 blue sources (lower 5 SEDs; first 5 table entries). The $24\mu m$ data points were down-weighted in these fits so that they would not throw off the fit in the 3-$5\mu m$ region which we are primarily concerned with here; MIR SEDs can have a wide range of shapes depending on details of geometry and astrophysics, which cannot be encapsulated in small libraries. The fitted redshifts range from 0.68 to 0.94, and the corresponding infrared luminosities range from log $L_{3-1000\mu m} =$ 10.3 to 11.3 $L_\odot$[1]; these are star forming galaxies and starbursts at moderate redshifts with moderate luminosities. The blue [3.6−4.5] region of the SED is only approximately fit, as anticipated, with deviations 0.8 to 2.2σ high for the $3.6\mu m$ points, and 4.3 to 7.9σ low for the $4.5\mu m$ data points (combined deviations of the [3.6−4.5] color from the template are given in the last column of Table 2). We present these fits as illustrative and not unique; fits at substantially different redshifts are possible with different combinations of templates and A_V values. If this phenomenon is confirmed as a real and substantial population with unusually blue 3-$5\mu m$ SEDs, ideal fits will require modified template modeling outside the current libraries. We note that the fitted redshifts for all of these objects are consistent with the hypothesis of a dominant population of red supergiants with strong CO absorption at $2.35\mu m$ redshifted into the $4.5\mu m$ band. It will be most interesting to discover whether Spitzer finds similarly blue colors in any regions within nearby galaxies, where the stellar populations and interstellar medium can be investigated in some detail.

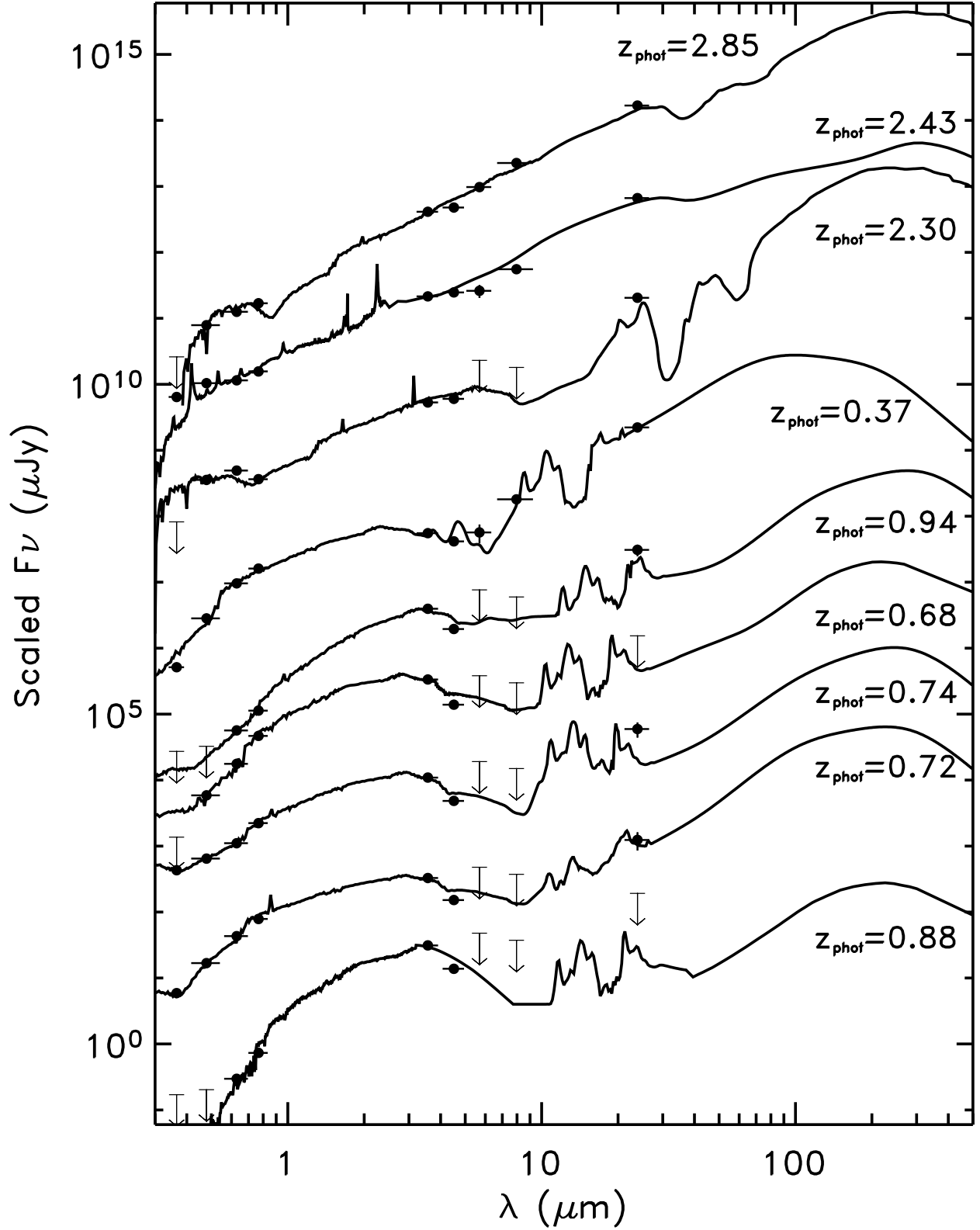[1] H_0=71 km/s/Mpc; Ω_m=0.27; $\Omega_\Lambda = 0.73$

Fig. 3.— SEDs for 5 sources with [3.6−4.5]< −0.3 (lower 5 SEDs) and 4 sources redder than [3.6−24]=7.5 mag. In most cases the uncertainties are smaller than the symbol sizes.

We have also selected all sources redder than $[3.6-24]=7.5$ mag. for investigation (see Figure 2), requiring a detection at S/N>5 at 24μm. Of 63 sources with $[3.6-24]>7.5$ mag., 42 were found to have valid colors this red on re-derivation of their fluxes by hand. The remainder are about evenly divided between sources for which more than one 3.6μm source likely contributes to the larger beam 24μm emission (a commonly expected situation due to the large difference in beam profiles), and spuriously low 3.6μm flux densities caused by latents or electronic offsets due to nearby bright stars. This latter category of anomalies at 3.6μm represents a $10/16075=0.06\%$ anomaly rate amongst the whole catalog, and 17% among the selected red sources. As for the unusually blue $[3.6-4.5]$ sources, a high anomaly rate amongst color outliers is not unanticipated.

Table 2.   Selected Sources with Unusually Blue [3.6−4.5] or Red [3.6−24] Colors

Name	RA J2000	Dec	z_{phot}	$L_{3-1000\mu m}$ $L_\odot$	A_V mag.	Template	Deviation, σ blue sources
SWIRE_J104513.3+585933	10 45 13.39	58 59 33.5	0.88	10.3	0.8	Sa	7.2
SWIRE_J104552.8+590600	10 45 52.86	59 06 00.8	0.72	11.3	1.0	Sd pec	7.2
SWIRE_J104657.3+590902	10 46 57.38	59 09 02.5	0.74	10.9	0.2	Sdm	4.6
SWIRE_J104743.7+591034	10 47 43.75	59 10 34.6	0.68	10.8	0.5	Sbc HII	8.4
SWIRE_J104436.8+591349	10 44 36.84	59 13 49.2	0.94	11.2	1.3	Sc strbst	6.2
SWIRE_J104616.0+591424	10 46 16.08	59 14 24.9	0.37	11.1	0.8	Im pec HII	$\cdots$
SWIRE_J104511.8+590121	10 45 11.88	59 01 21.6	2.30	13.4	0.2	HII	$\cdots$
SWIRE_J104613.4+585941	10 46 13.44	58 59 41.3	2.43	13.2	1.1	QSO	$\cdots$
SWIRE_J104700.2+590107	10 47 00.20	59 01 07.6	2.85	13.7	0.3	Sy1	$\cdots$

The best fit redshifts for 4 representative red sources (Figure 3 upper 4 SEDs & Table 2 last 4 entries) range from 0.37 to 2.85, with a luminosity range of log $L_{3-1000\mu m}$=11.1 to 13.7 $L_{\odot}$. It is very difficult to obtain unique fits for some objects of this type owing to the flatness of the SEDs and the limited number of data points, and these fits should be regarded as illustrative only, pending a thorough analysis of the possible range of templates, redshifts and luminosities that can fit each of these sources. These objects appear to be starbursts, ULIRGs and AGN with a wider redshift and luminosity range than the blue sources in Figure 3, including some z>2 objects with luminosities in the hyperluminous object (HyLIRG) range. SWIRE is expected to be particularly sensitive to high-redshift IR-luminous AGN, which are expected to be bright in the very sensitive 24μm band due to warm circumnuclear dust. The high-redshift volume density of HyLIRGs will be important for models for the early formation of massive systems in the Universe. Spitzer IRS spectroscopy may prove essential for determining redshifts and excitations for the reddest, optically-faintest, systems.
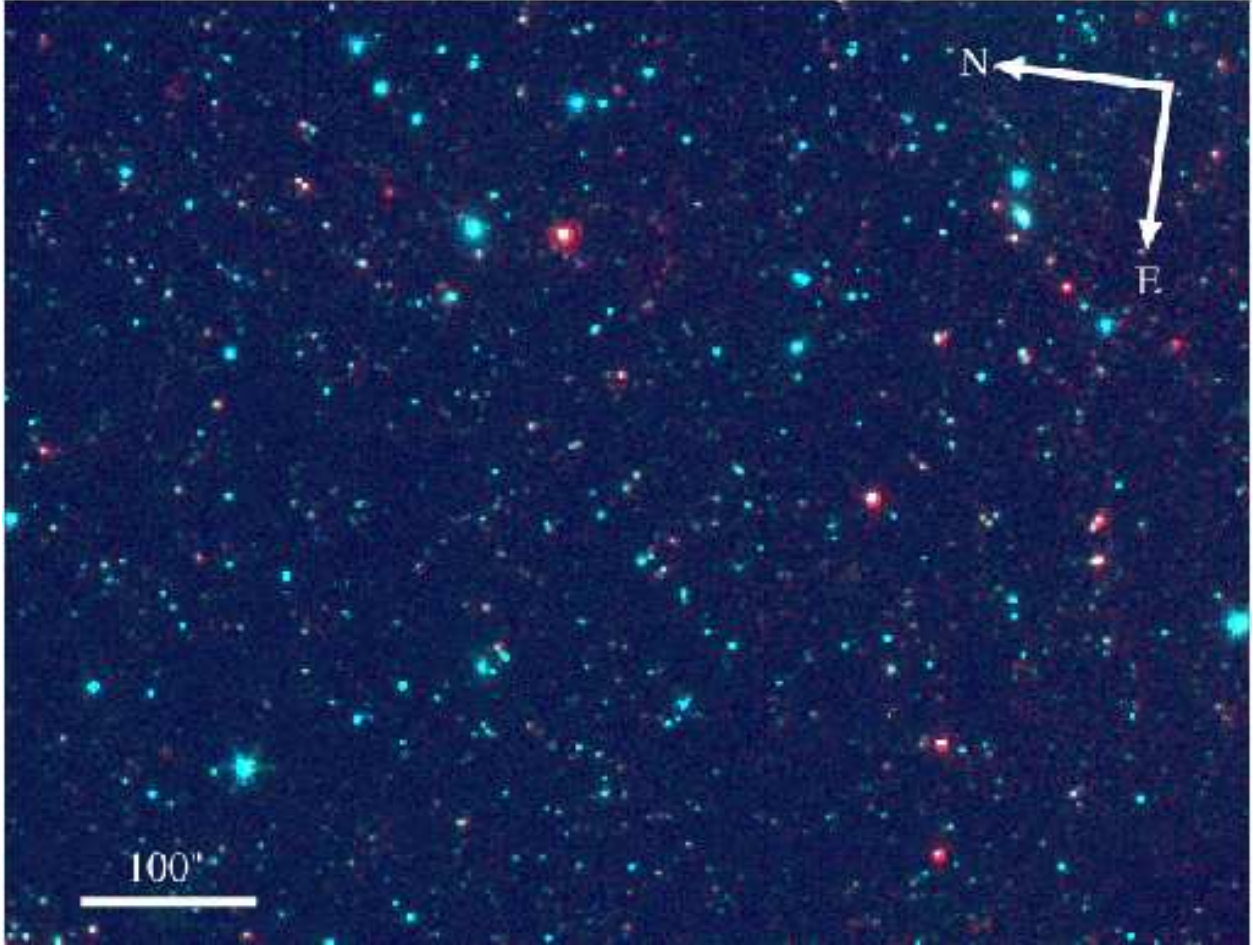
Fig. 4.— Plate 1: 3-color image of $\sim$0.03 sq. deg of the SWIRE Lockman validation field, centered at $10^h47^m32.67^s$, $59^d07^m16.3^s$: 3.6μm (blue), 4.5μm (green), 24μm (red).

REFERENCES

Andreani P., Cristiani S., Grazian A., La Franca F., Goldschmidt P. 2003 AJ, 125, 444

Babbedge, T.S., Rowan-Robinson, M., Gonzalez-Solares, E., Polletta, M. et al., 2004, MNRAS, submitted

Bahcall, J.N., & Soneira, R.M., 1980, ApJS, 44,73

Beichman, C., Cutri, R., Jarrett, T., Steining, R. & Skrutski, M. 2003, AJ, 125, 252

Berta S., Fritz J., Franceschini A., Bressan A., Lonsdale C. 2004, A&A, in press

Bolzonella M., Miralles J.-M. and Pelló R. 2000, A&A, 363, 476

Farrah, D., Fox, M., Efstathiou, A., Afonso, J., Clements, D. & Rowan-Robinson, M. 2003, MNRAS, 343, 585

Gregg, M.D., Lacy, M.m White, R.L., Glikman, E., Helfand, D., Becker, R.H. and Brotherton, M.S. 2002, ApJ, 564, 133

Jarrett, T. H., Dickman, R. L., and Herbst, W., 1994, ApJ, 424, 852

Lonsdale, C. et al., 2003, PASP, 115, 897

Oliver, S. et al. 2004, ApJ, this volume

Rhoads, J. 1997, in "Extragalactic Astronomy in the Infrared", Paris: Edition Frontieres, ed. G. Mamon, T. X. Thuan, J. Tran Than Van, p 45.

Rowan-Robinson, M. 2003, MNRAS, 345, 819

Shupe, J. et al. 2004, in preparation

Silva, L., Granato, G.L., Bressan, A., Danese, L. 1998, ApJ, 509, 103

Surace, J. et al. 2004, in preparation

Xu, C. K., Lonsdale, C.J., Shupe, D.L., Franceschini, A., Martin, C., & Schiminovich, D. 2003, ApJ, 587, 90